

Influence of air-abrasion executed with polyacrylic acid-Bioglass 45S5 on the bonding performance of a resin-modified glass ionomer cement

Salvatore Sauro¹, Timothy F. Watson¹, Ian Thompson¹, Manuel Toledano², Cesare Nucci³, Avijit Banerjee^{1,4}

¹Biomaterials, Biomimetics & Biophotonics Department, King's College London Dental Institute at Guy's Hospital, King's Health Partners, London, UK; ²Dental Materials, School of Dentistry, University of Granada, Colegio Máximo, Campus de Cartuja, Granada, Spain; ³Department of Dental Sciences, Alma Mater Studiorum, University of Bologna, Bologna, Italy; ⁴Department of Cariology & Operative Dentistry King's College London Dental Institute, Tower Wing Guy's Dental Hospital London, UK

Sauro S, Watson TF, Thompson I, Toledano M, Nucci C, Banerjee A. Influence of air-abrasion executed with polyacrylic acid-Bioglass 45S5 on the bonding performance of a resin-modified glass ionomer cement.

Eur J Oral Sci 2012; 00: 000–000. © 2012 Eur J Oral Sci

The aim of this study was to test the microtensile bond strength (μ TBS), after 6 months of storage in PBS, of a resin-modified glass ionomer cement (RMGIC) bonded to dentine pretreated with Bioglass 45S5 (BAG) using various etching and air-abrasion techniques. The RMGIC (GC Fuji II LC) was applied onto differently treated dentine surfaces followed by light curing for 30s. The specimens were cut into matchsticks with cross-sectional areas of 0.9 mm². The μ TBS of the specimens was measured after 24 h or 6 months of storage in PBS and the results were statistically analysed using two-way ANOVA and the Student–Newman–Keuls test ($\alpha = 0.05$). Further RMGIC-bonded dentine specimens were used for interfacial characterization, microporosity, and nanoleakage analyses by confocal microscopy. The RMGIC–dentine interface layer showed no water absorption after 6 months of storage in PBS except for the interdiffusion layer of the silicon carbide (SiC)-abraded/polyacrylic acid (PAA)-etched bonded dentine. The RMGIC applied onto dentine air-abraded with BAG/H₂O only or with BAG/PAA-fluid followed by etching procedures (10% PAA gel) showed no statistically significant reduction in μ TBS after 6 months of storage in PBS. The abrasion procedures performed using BAG in combination with PAA might be a suitable strategy to enhance the bonding durability and the healing ability of RMGIC bonded to dentine.

Dr Salvatore Sauro, Dental Biomaterials Science, King's College London Dental Institute, Floor 17 Guy's Tower, London SE1 9RT, UK

Telefax: +44–207 188 1823
E-mail: salvatore.sauro@kcl.ac.uk

Key words: air-abrasion; Bioglass 45S5; bonded-dentine durability, microtensile bond strength, confocal microscopy; polyacrylic acid; resin-modified glass ionomer cements

Accepted for publication November 2011

The contemporary idea of minimally invasive operative treatment is to perform therapeutic restorations that may combat the carious process and remineralize the dental hard tissues (1–3). The stabilization of the carious lesion and the creation of an optimal environment to repair the demineralized dental hard tissues are of primary importance to achieve these aims (3–5).

Bioglass 45S5 (BAG) is a bioactive calcium/sodium phosphate-phyllsilicate that reacts with body fluids, encouraging the formation of hydroxyapatite [Ca₁₀(PO₄)₆(OH)₂] and the remineralization of dental hard tissues (6–9). It is used in dentistry as a substitute for alumina powder in air-abrasion systems as an alternative to traditional hand-pieces in removing the dental hard tissues (i.e. enamel, dentine, and cementum) (10, 11). The clinical use of BAG within the air-abrasion systems has advantages, including the absence of pain during the operative procedures and the opportunity to prepare ultraconservative cavities with rounded internal line

angles, thus minimizing the contraction stress of composites (10). The specific formulation of BAG created for air-abrasion procedures has a Young's modulus of 35 GPa and Vickers' hardness of 458 VHN, which are significantly lower than those for alumina (380 GPa and 2,300 VHN, respectively) but very similar to those of mineralized dentine. These physical attributes may allow for the selective removal of carious dentine (10, 11).

Studies have demonstrated the ability of glass ionomer cements (GICs) to induce crystal growth in microspaces within the interface of the restoration after long-term storage in water (12, 13), and the chemical composition of these crystals is similar to that of dental hard tissue (14, 15). Although GICs may have reduced mechanical characteristics (i.e. wear resistance, brittleness, and low-bond strength) compared with resin adhesives and composites, they have excellent handling properties and, unlike resin adhesives and composites, are less sensitive to the moist clinical conditions present during bonding

procedures (16–20). Glass ionomer cements are widely used in conservative dentistry as a result of their unique anticariogenic/antibacterial properties and because they adhere chemically to teeth as a result of ion release and bond formation (21–23). However, light-cured resin-modified glass ionomer cements (RMGICs) have been developed with the intent to combine the properties of GICs with the mechanical properties of resin polymers (21, 24). They consist of a fluoro-alumino silicate (FAS) powder, similar to that of conventional glass ionomers, combined with monomers [i.e. 2-hydroxyethyl methacrylate (HEMA), triethyleneglycol dimethacrylate (TEGDMA), and urethane dimethacrylate (UDMA)] and photo-initiators as the resin component (22, 23). The setting process of these materials occurs by free-radical polymerization with a subsequent acid–base reaction between the polycarboxylic acids and the FAS (22).

This operative combination between air-abrasive procedures performed with BAG and subsequent restoration using RMGICs could be a strategy to satisfy the contemporary idea of minimally invasive operative dentistry. However, this combination has never been tested and there is no information on the effect of air-abrasion performed with BAG under an H₂O or polyacrylic acid (PAA) shroud on the bonding performance of resin-modified GICs.

The aim of this study was to test the microtensile bond strength (μ TBS), after 6 months of storage in PBS, of an RMGIC bonded to dentine pretreated with BAG using various air-abrasion and etching techniques. The interfacial characteristics, micropermeability, and nanoleakage of the bonded interfaces were evaluated using confocal microscopy. The null hypothesis to be tested was that the different etching and air-abrasion techniques do not influence the μ TBS and the ultramorphology of the RMGIC-bonded dentine interfaces after 24 h or 6 months of storage in PBS.

Material and methods

Specimen preparation

Caries-free molars from 20- to 40-yr-old human subjects, extracted for periodontal or orthodontic reasons under a

protocol approved by an Institutional Review Board of the King's College London, Dental Institute (London, UK) (ref. 10/H0721/55), were used in this study. The teeth were stored in deionized water (pH 7.1) at 4°C for no longer than 1 month. Coronal dentine specimens were prepared by sectioning the roots 1 mm beneath the cemento–enamel junction (CEJ) using a diamond-embedded blade (high concentration XL 12205; Benetec, London, UK) mounted on a hard-tissue microtome (Isomet 11/1180; Buehler, Coventry, UK). A subsequent parallel cut was performed to remove the occlusal enamel and expose the middle coronal dentine. The dentine surface was immediately polished with 180-grit silicon carbide (SiC) paper for 1 min under continuous water irrigation to create a standard and more clinically relevant smear layer (24). The specimens were divided into experimental groups and subgroups, as shown in Table 1.

Experimental design: dentine pretreatment and bonding procedures

The use of air-abrasion devices at specific air pressure (> 300 MPa) for more than 30 s may tend to cause BAG to embed in the dentine surface and inside the dentinal tubules (9). In this study the dentine specimens were air-abraded with BAG (particle size: 30–60–90 μ m) using two different approaches: (i) in combination with deionized H₂O (air-abrasion BAG control); and (ii) in combination with a 10% PAA fluid (air-abrasion BAG experimental). In this latter technique the water in the air-abrasion device was replaced with a 10 wt% PAA (relative molecular mass = 1800; Sigma Chemicals, Gillingham, Dorset, UK) water solution (pH ~2.0) in order to increase the probability of BAG particles embedding in dentine. The pH of the 10 wt% PAA solution was measured using a professional pH electrode (Mettler-Toledo, Leicester, UK). Moreover, the pH values of the BAG/H₂O and BAG/PAA-fluid solutions (15 ml) sprayed during air-abrasion procedures were also evaluated (Table 2). The air-abrasion system used to deliver the BAG onto the dentine surface was an Aquacut Quattro (VELOPEX International, London, UK), which was used at an air pressure of 5 bar (500 MPa) for 1 min at a distance of 1 cm from the dentine surface. The experimental design required the abraded dentine surface to be conditioned with 10% PAA gel (pH ~1.9) for 20 s using the Fuji II LC liquid (GC, Newport Pagnell, UK) and rinsed with water for 20 s (etching control) or left unconditioned (etching experimental).

Table 1

Experimental design and number of teeth used in each experimental group

Groups	Dentine treatments	Dentine etching (10% PAA gel)*	Subgroups (μ TBS/confocal-micropermeability /confocal nanoleakage) inPBS	
			24 h storage in PBS	6-months storage in PBS
1	SiC paper	No	[5/3/3]	[5/3/3]
2	SiC paper	Yes	[5/3/3]	[5/3/3]
3	Air-abrasion: BAG/H ₂ O	No	[5/3/3]	[5/3/3]
4	Air-abrasion: BAG/H ₂ O	Yes	[5/3/3]	[5/3/3]
5	Air-abrasion: BAG/10% PAA-fluid	No	[5/3/3]	[5/3/3]
6	Air-abrasion: BAG/10% PAA-fluid	Yes	[5/3/3]	[5/3/3]

*GC Fuji conditioner (GC, Newport Pagnell, UK). BAG, Bioglass 45S5; PAA, polyacrylic acid; SiC, silicon carbide; μ TBS, microtensile bond strength.

Number of teeth used for μ TBS/confocal-IP /confocal nanoleakage.

Table 2

Brand name, chemical composition, and application mode of products used for pretreatments and bonding procedures

Brand name	Chemical composition	Solutions (and their pH) used during air-abrasion procedures
GC Fuji II LC*	Powder: fluoro-alumino silicate glass Liquid: PAA, tartaric acid, 2-hydroxyethyl methacrylate (HEMA), dimethacrylate, H ₂ O, camphorquinone (CQ)	10% PAA gel (pH ~1.9)
GC Fuji conditioner*	10% PAA gel	10% PAA solution (pH ~2.0)
PAA-fluid air-abrasion†	10wt% PAA water solution	BAG/H ₂ O‡ (pH ~9.4)
Bioglass 45S5 (Sylc)§	46.1 mol% SiO ₂ , 26.9 mol% CaO, 24.4 mol% Na ₂ O, and 2.5 mol% P ₂ O ₅ (particle size: 30–60–90 µm)	BAG/PAA-fluid‡ (pH ~6.8)

BAG, Bioglass 45S5; PAA, polyacrylic acid.

*GC United Kingdom, (Newport Pagnell, UK).

†Sigma Chemicals (Gillingham, Dorset, UK).

‡pH of the BAG/H₂O or BAG/PAA-fluid solutions sprayed during air-abrasion.

§Sylc (OSspray, London, UK).

Overall, six groups were created in this experimental design.

Group 1. Specimens were abraded using 180-grit SiC abrasive paper (1 min) under continuous irrigation, followed by a water rinse (20 s) and air-drying (2 s), and then bonding with light-cured RMGIC/resin composite, as previously described.

Group 2. Specimens were abraded with 180-grit SiC abrasive paper (1 min), etched with 10% PAA gel for 20 s (GC), rinsed with water (20 s), dried, and restored with light-cured RMGIC/composite. This was the second control where the RMGIC was used according to the manufacturer's instructions.

Group 3. Specimens were air-abraded with BAG particles under a continuous water shroud (1 min), rinsed with water (20 s), dried, and restored with light-cured RMGIC/composite.

Group 4. Specimens were air-abraded with BAG particles under a continuous water shroud (1 min), rinsed with water (20 s), etched with 10% PAA (20 s), rinsed with water (20 s), dried, and restored with light-cured RMGIC.

Group 5. Specimens were air-abraded with BAG under a continuous PAA shroud (10% PAA water solution), rinsed with water (20 s), and then restored with light-cured RMGIC.

Group 6. Specimens were air-abraded with BAG under a continuous PAA shroud (10% PAA for 1 min), acid-etched using 10% PAA gel for 20 s, rinsed with water (20 s), and then restored with light-cured RMGIC.

The bonding procedures were performed by applying two consecutive coats of the RMGIC (GC Fuji II LC; GC) to the differently treated dentine surfaces followed by light curing for 30 s with a light-curing unit with a blue light source (470 nm, 600 mW/cm², Optilux VLC; Demetron Research, Danbury, CT, USA). A flowable resin composite (Filtek Supreme XT, 3 M ESPE, St. Paul, MN, USA) was finally placed incrementally in 1-mm layers to create a 5-mm build-up. Each layer was light-cured for 20 s with a final burst of 40 s.

The specimens were stored in PBS [composition: 0.103 g l⁻¹ of CaCl₂, 0.019 g l⁻¹ of MgCl₂·6H₂O, 0.544 g l⁻¹ of KH₂PO₄, 30 g l⁻¹ of KCl, and 4.77 HEPES (acid) buffer, pH 7.4 (9)] at 37°C for 24 h or 6 months, depending on the experimental group.

µTBS test

The specimens from each group (Table 1) were sectioned using a hard-tissue microtome (Isomet 11/1180; Buehler) in both X and Y directions across the bonding interface, obtaining matchsticks with cross-sectional areas of 0.9 mm², which were stored in PBS for 24 h or 6 months. The bonded-dentine beams situated peripherally, including enamel, were excluded from the µTBS test. Half of the beams suitable for the µTBS test were analyzed immediately after storage in PBS for 24 h or 6 months (Table 3). The µTBS tests were performed using a customized microtensile jig on a linear actuator (SMAC Europe, Horsham, West Sussex, UK) with LAC-1 (a high-speed controller single axis with a built-in amplifier) and a LAL300 linear actuator that has a stroke length of 50 mm with peak force of 250 N and a displacement resolution of 0.5 mm. Bond strength data were analysed statistically by two-way ANOVA including interactions between factors, using µTBS as a dependent variable. Dentine surface treatment and PBS storage were considered as independent variables. Post-hoc multiple comparisons were performed using the Student–Newman–Keuls test. Statistical significance was set at $\alpha = 0.05$. Modes of failure were classified as percentage of adhesive (A) or mixed (M) or cohesive (C) failures when the failed bonds were examined at 30× magnification by stereoscopic microscopy.

Confocal microscopy evaluation

Further dentine specimens were bonded with the RMGIC, as previously described. Rhodamine B powder (Sigma Chemicals) was added (at 0.1 wt%) to the GC Fuji II LC liquid which was immediately mixed with the GC Fuji II LC powder according to the manufacturer's instructions (Table 2). Confocal microscopy was employed to ascertain the interfacial characteristics, micropermeability, and nanoleakage (Table 1) in order to investigate the main morphological details of the bonded-dentine interfaces. The pulp chambers of the bonded-dentine specimens designated for the micropermeability evaluation were filled with 1 wt% aqueous fluorescein dye solution for 3 h (25, 26) and subsequently rinsed with copious amounts of water in an ultrasonic bath for 2 min. The specimens were sliced vertically into 1-mm slabs using a slow-speed water-cooled

Table 3

Microtensile bond strength (μ TBS), number of sticks tested, and percentage of failure modes

Groups	Dentine treatments	PBS storage	
		24 h	6 months
1	SiC-abrasion (56/4)	26.6 \pm 19.6 ^{A*} (25/1) [55/45/5]	13.8 \pm 9.6 ^a (23/3) [35/55/10]
2	SiC-abrasion/PAA-etch (52/4)	37.1 \pm 16.6 ^{C*} (26/0) [60/35/5]	24.8 \pm 13.9 ^d (24/2) [55/45/5]
3	Air-abrasion/BAG-H ₂ O (50/3)	15.5 \pm 17.3 ^B (25/2) [65/30/5]	12.5 \pm 17.1 ^a (26/1) [60/40/0]
4	Air-abrasion BAG-H ₂ O/PAA-etch (56/2)	35.2 \pm 17.3 ^{C*} (30/0) [70/5/25]	18.8 \pm 10.9 ^c (28/2) [55/40/5]
5	Air-abrasion BAG-PAA-fluid (54/5)	27.6 \pm 17.6 ^{A*} (27/0) [65/35/5]	14.1 \pm 15.1 ^a (27/0) [50/45/5]
6	Air-abrasion BAG-PAA/PAA-etch (50/3)	36.5 \pm 19.7 ^C (25/0) [65/5/35]	32.1 \pm 13.8 ^b (25/0) [75/10/15]

The results show the mean \pm SD of the μ TBS (MPa) to dentine when resin-modified glass ionomer cement (RMGIC) was applied after different dentine pretreatments. Also given are the total number of beams (intact sticks/prefailed sticks) in the dentine treatment groups and the number of beams (intact sticks/prefailed sticks) and percentage of failure modes [mix/adhesive/cohesive] in the PBS storage groups. The same letter indicates no differences in columns with different dentine treatments maintained in the same storage media. The (*) indicates differences in rows for different PBS storage times ($P > 0.05$).

BAG, Bioglass 45S5; PAA, polyacrylic acid; SiC, silicon carbide.

diamond saw (Labcut; Agar Scientific, Stansted, UK) and polished using 1,200-grit SiC paper for 30 s followed by a further rinse in an ultrasonic bath (1 min). The specimens designated for the nanoleakage evaluation were vertically sectioned into 0.9-mm slabs and coated with two layers of fast-setting nail varnish, applied 1 mm from the bonded interfaces. Before these slabs could become dehydrated, they were immersed immediately in 1 wt% aqueous fluorescein dye solution for 24 h. The micropermeability and the nanoleakage along the interfaces were examined using (i) a confocal laser scanning microscope (Leica SP2 CLSM; Leica, Heidelberg, Germany), equipped with a 63 \times /1.4 NA oil-immersion lens and a 514 nm argon/helium ion laser, and (ii) a tandem scanning confocal microscope (Noran Instruments, Middleton, WI, USA) equipped with a 100 \times /1.4 NA oil-immersion objective. Confocal laser scanning microscopy reflection and fluorescence images were obtained with a 1- μ m z -step to section optically the specimens to a depth of up to 20 μ m below the surface. The z -axis scan of the interface surface was arbitrarily pseudo-coloured by two selected operators for better exposure and compiled into both single and topographic projections using LEICA SP2 CLSM image-processing software (Leica). The configuration of the system was standardized and used at the same settings for the entire investigation. Each dentine interface was completely investigated and then five optical images were randomly captured. Micrographs representing the most common features of micropermeability and nanoleakage observed along the bonded interfaces were captured and recorded.

Results

μ TBS test

Dentine surface treatments and storage time in PBS influenced the μ TBS results ($P < 0.01$). Interactions between factors were also significant ($F = 162.35$; $P < 0.05$). The μ TBS values (mean \pm SD) of the bonded-dentine interfaces tested in this study are shown in Table 3.

The RMGIC applied on an intact smear layer (Group 1) with no prior etching (10% PAA gel) attained μ TBS values of 26.6 \pm 19.6 MPa and 13.8 \pm 9.6 MPa after 24 h and 6 months, respectively, of storage in PBS.

When the RMGIC was applied according to the manufacturer's instructions (Group 2) using the 10% PAA gel to etch the dentine, the μ TBS was higher in the control specimens after 24 h of storage in PBS (up to 37.1 \pm 16.6 MPa) but showed a significant decrease ($P < 0.05$) (to 24.8 \pm 13.9 MPa) after 6 months of storage in PBS. Although the μ TBS values achieved with the RMGIC applied on BAG/H₂O air-abraded dentine (Group 3) were lowest after 24 h of storage in PBS (15.5 \pm 17.3 MPa), no statistically significant reduction in μ TBS was observed after 6 months of storage in PBS (12.5 \pm 17.1 MPa). Conversely, when the air-abrasion procedures were performed using BAG/H₂O followed by etching (Group 4) or using BAG/PAA-fluid followed by no etching (Group 5), a statistically significant reduction in μ TBS was observed after 6 months of storage in PBS. No statistically significant reduction in μ TBS after 6 months of storage in PBS was observed when the RMGIC was applied on a dentine surface air-abraded with BAG/PAA-fluid and subsequently etched using the PAA gel-etchant (Group 6).

Confocal microscopy evaluation

The tandem scanning confocal microscopy (TSM) and confocal laser scanning microscopy (CLSM) interfacial characterization, micropermeability, and nanoleakage analyses performed after 24 h of storage in PBS showed important features regarding the application of RMGIC onto dentine that had received different pretreatments (Figs 1, 2 and 3).

For instance, a distinguishing layer free from FAS glass fillers between dentine and the proper RMGIC layer and evident water sorption via dentinal tubules (micropermeability) were observed in all the specimens after 24 h of storage in PBS (Fig. 1). The RMGIC bonded to dentine treated with BAG fluid showed a strong reflective signal from BAG particles obliterating the dentinal tubules (Fig. 1B). The nanoleakage analysis of RMGIC-bonded dentine indicated that both the FAS-free and RMGIC layer of all the specimens were able to take up fluids after 24 h of storage in PBS (Fig. 1F).

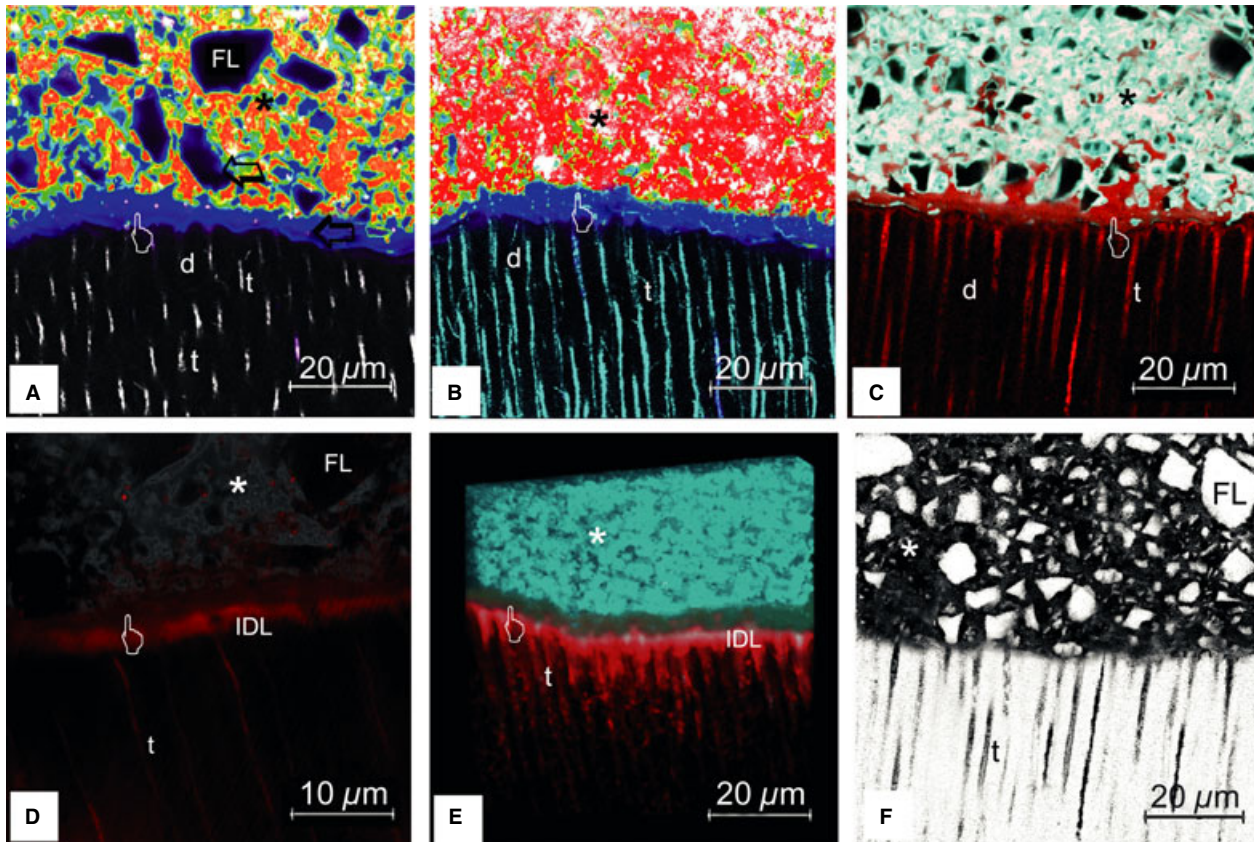


Fig. 1. Confocal laser scanning microscopy (CLSM) and tandem scanning confocal microscopy (TSM) images showing the interfacial characterization, micropermeability, and nanoleakage of the different bond–dentine specimens investigated in this study after storage in PBS for 24 h. (A) The CLSM projection image (reflection/fluorescence) exemplifies the interfacial characteristics of the bond–dentine interface created by application of the resin-modified glass ionomer cement (RMGIC) onto dentine air-abraded with Bioglass and H₂O. It is possible to observe a layer free of fluoro-alumino silicate (FAS) filler (pointer) located between the dentine (d) and the proper RMGIC layer (*). Note the presence of the FAS lacunas (FLs). The blue pseudo-colours around the FLs and within the glass-free layer may indicate the accumulation of 2-hydroxyethyl methacrylate (HEMA) and the presence of a reactive silica gel layer created by the reaction of the polycarboxylic acids and the FAS particles (arrows). (B) The three-dimensional (3D) CLSM single projection image (reflection/fluorescence) shows the interfacial characteristics of the bonded–dentine interface created by application of the RMGIC onto dentine air-abraded with Bioglass and polyacrylic acid (PAA) fluid and etched with 10% PAA gel. It is possible to observe a layer free of glass filler (pointer) between the dentine (d) and the proper RMGIC layer (*). Note the reflective signal of Bioglass 45S5 (BAG) from the obliterated dentinal tubules (t). The same reflective signal observed in the proper RMGIC layer (*) indicates the presence of FAS glass (a white pseudo-colour). The red and yellow pseudo-colours in the proper RMGIC layer (*) may indicate resin components of the RMGIC. (C) Bonded–dentine interface created by application of the RMGIC onto dentine air-abraded with Bioglass and PAA fluid. This CLSM single projection image (reflection/fluorescence) shows how the layer free of FAS (pointer), located between the dentine (d) and the proper RMGIC layer (*), is affected by fluid uptake (rhodamine B) via dentinal tubules (micropermeability). Note the absence of an evident interdiffusion layer (IDL) within the RMGIC–dentine interface. (D) Bonded–dentine interface obtained by applying the RMGIC onto sound dentine according to the manufacturer’s instructions (etched with PAA etching gel). It is possible to distinguish dye diffusion (micropermeability) through dentinal tubules (t) to the glass-free layer (pointer) located between the IDL of the dentine (d) and the proper RMGIC layer (*). (E) Representative images of the RMGIC–dentine interface obtained by applying RMGIC onto dentine air-abraded with Bioglass/PAA-fluid and etched using 10% PAA gel. An IDL is clearly visible. Moreover, it is possible to distinguish dye diffusion (micropermeability) through dentinal tubules (t) to the glass-free layer (pointer) located between the dentine (d) and the proper RMGIC (*). (F) The CLSM single projection image (fluorescence) shows nanoleakage along the interface of the dentine bonded with achieved following application of RMGIC onto dentine air-abraded with Bioglass and PAA fluid. Penetration of the fluorescence dye (rhodamine B) within the entire RMGIC layer (*) and into the dentinal tubules (t) is shown. Note the absence of an evident IDL.

In contrast, the RMGIC-bonded specimens investigated after 6 months of storage in PBS presented completely different micropermeability and nanoleakage scenarios (Fig. 2). For instance, the resin–dentine interface showing residual dye penetration within the interdiffusion layer (IDL) was restricted to that created when the RMGIC was applied onto the SiC-treated/PAA-etched dentine (Group 2) (Figs 2A and 3A). Conversely,

the bonded–dentine interfaces created by applying the RMGIC onto BAG/H₂O air-abraded dentine (Groups 3 and 4) were characterized by dye diffusion (micropermeability) into the dentinal tubules with no uptake within the bonding interface (Fig. 2D,E). Likewise, the BAG/PAA-fluid air-abraded dentine bonded with RMGIC (Groups 5 and 6) showed dye micropermeability only into the dentinal tubules and no water

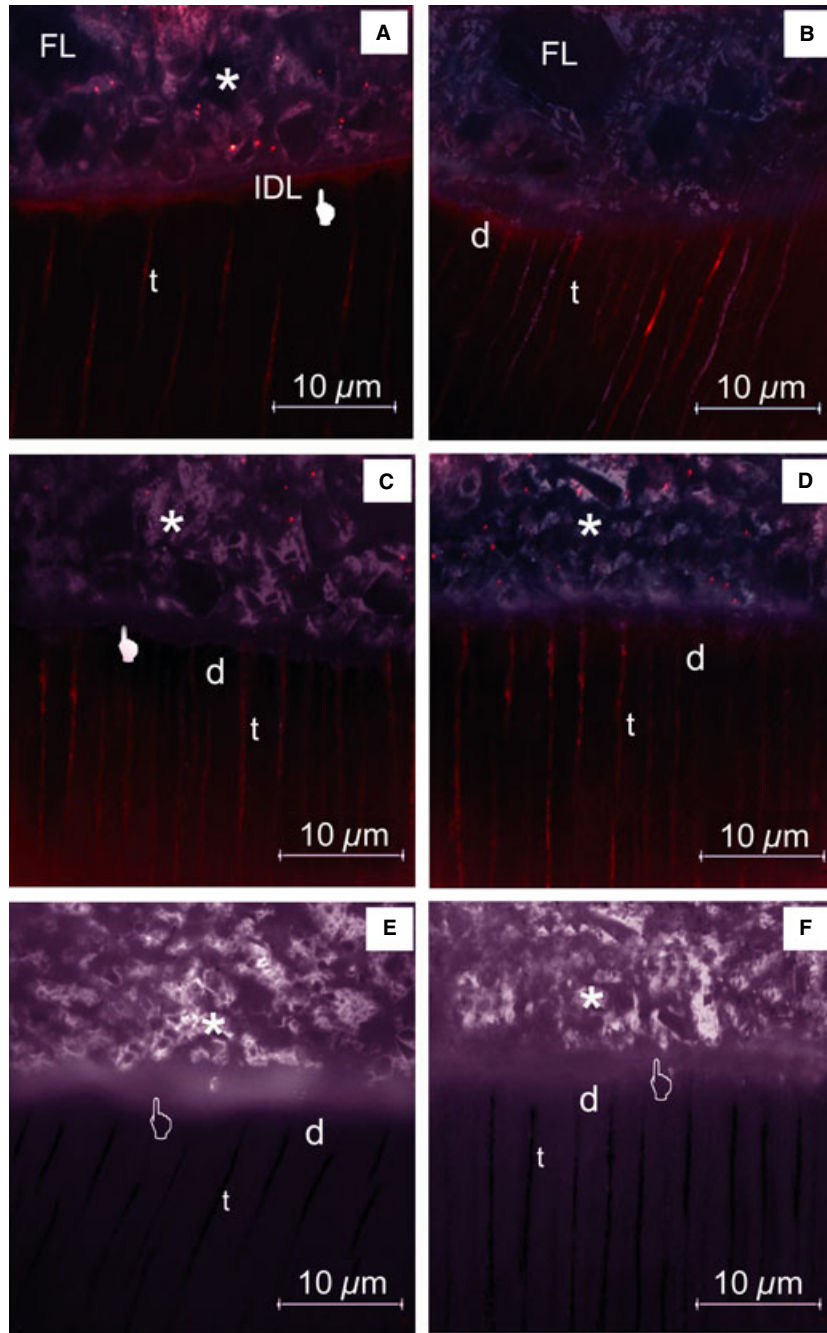


Fig. 2. Tandem scanning confocal microscopy (TSM) confocal images showing the interfacial characterization, micropermeability, and nanoleakage of the different bonded-dentine specimens investigated in this study after 6 months of storage in PBS. (A) The image (reflection/fluorescence) shows the bond–dentine interface created by application of the resin-modified glass ionomer cement (RMGIC) onto silicon carbide (SiC)-abraded, polyacrylic acid (PAA)-gel-etched dentine (Group 2). It is possible to observe clear diffusion of dye (micropermeability) into the dentinal tubules (t) with no uptake within the bonding interface between the RMGIC (*) and dentine (d). IDL, interdiffusion layer. (B) The image (reflection/fluorescence) exemplifies the bond–dentine interface created following the application of RMGIC onto dentine air-abraded with Bioglass/PAA-fluid and etched with 10% PAA gel. It is possible to observe dye diffusion (micropermeability) into the dentine tubules (t) with no uptake within the bonding interface between the RMGIC (*) and dentine (d). Fluoro-alumino silicate lacunas (FLs) are also visible. (C) The image (reflection/fluorescence) shows the bond–dentine interface created using the RMGIC applied onto dentine air-abraded with Bioglass and PAA fluid. Dye penetration (rhodamine B) is only visible along the dentine tubules (t). The bonding interface between the RMGIC (*) and dentine (d) is free from fluid dye absorption. (D) The image (reflection/fluorescence) exemplifies the bonded-dentine interface created using the RMGIC applied according to the manufacturer’s instructions onto a sound smear layer. In this particular case it is possible to see dye penetration both into the dentine tubules (t) and within the IDL. Images (E) and (F) are representative images showing nanoleakage along the interface created by application of RMGIC onto dentine air-abraded with Bioglass/H₂O (E) or Bioglass/PAA-fluid (F) and subsequently etched using a 10% PAA etching gel. It is important to note the absence of dye penetration both within the RMGIC–dentine interface and within the proper RMGIC layer (*) except the dentinal tubules (black pseudo-colours).

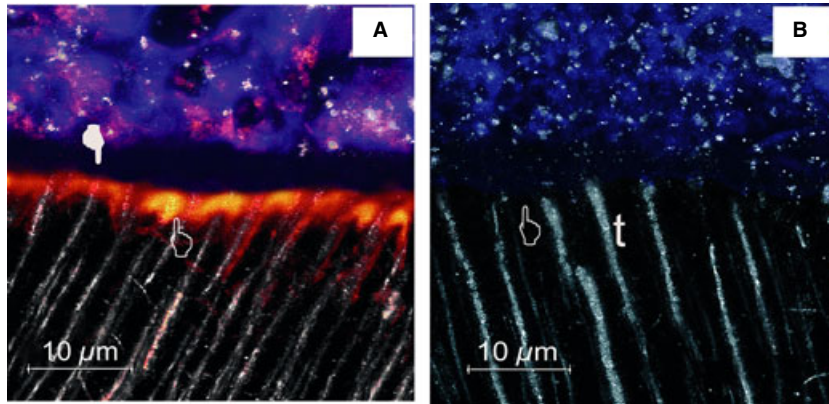


Fig. 3. (A) The three-dimensional (3D) single projection image (reflection/fluorescence) shows dye diffusion within the porous interdiffusion layer (IDL) of the bond–dentine interface created using the resin-modified glass ionomer cement (RMGIC) applied, according to the manufacturer’s instructions, onto a smear layer and stored in PBS for 6 months (see-through pointer). The absence of water absorption with the glass filler-free layer (white pointer) is indicated. (B) The 3D single projection image (reflection/fluorescence) shows no dye diffusion within the bond–dentine interface created using the RMGIC applied onto dentine abraded with Bioglass 45S5 (BAG) and stored in PBS for 6 months (see-through pointer). The absence of water absorption within the glass filler-free layer (white pointer) is also indicated.

sorption within the IDL layer (Fig. 2B,C). The absence of water uptake within the interface of the BAG/H₂O (Fig. 2E) or BAG/PAA air-abraded and PAA-etched dentine (Fig. 2F) was confirmed by the nanoleakage results, which showed diffusion of dye into the dentinal tubules only.

Discussion

The null hypothesis was rejected because the different etching and Bioglass air-abrasion dentine pretreatments influenced the μ TBS and the interface ultramorphology after storage in PBS for both 24 h and 6 months.

Micropermeability and nanoleakage evaluations were used to assess the RMGIC-bonded dentine interface avoiding unexpected artefacts or false results induced by the experimental design used in this study. Indeed, the micropermeability results mainly showed that water permeation within the bonded-dentine interface was limited to the RMGIC–dentine zone (Fig. 1C,D), while nanoleakage data clearly showed water sorption within the entire RMGIC layer after 24 h of storage in PBS (Fig. 1F). Conversely, no dye permeation was detected within the RMGIC-bonded dentine interface after 6 months of storage in PBS when tested for both nanoleakage and micropermeability. These findings were the result of important ultramorphological changes induced by the different etching and dentine pretreatments on the RMGIC-bonded dentine interface after 6 months of storage in PBS. For instance, the PAA-etched dentine showed a shallow demineralization layer (3–5 μ m) within the bonding interface (Figs 2D and 3A). In contrast, the air-abrasion procedures performed using BAG in combination with H₂O or 10% PAA fluid induced no evident demineralization of the dentine surface (Fig. 1F) owing to their neutral and alkaline pH values, respectively (Table 2). A distinguishing layer free of FAS glass filler, characterized by

dye uptake from the pulp chamber, was always observed in all the specimens (Fig. 1A,B). This layer is produced by the reaction of the polycarboxylic acids and FAS. SIDHU & WATSON (22) stated that the water-permeable ‘structureless’ (non-particulate) layer localized at the interfacial region between the dentine and the RMGIC layer may be caused by the accretion of poly-HEMA and a PAA-rich silica-gel layer. The authors also classified this part of the interface as the ‘absorption layer’. The water sorption ability of an RMGIC is a key factor for the ion-release properties that depend on specific factors, including resin monomers, filler type, and degree of monomer conversion (23); RMGIC and conventional GICs have greater water uptake than composites or resin composites (22, 25, 26). This absorption layer was also classified as a ‘self-healing’ feature that may compensate for the setting shrinkage and maintains the fit of the RMGIC after initial polymerization shrinkage has occurred (22, 26). It is suggested that this zone of the bond–dentine interface may be considered as a ‘reactive layer’ owing to the ultramorphological changes observed after 6 months of storage in PBS. Indeed, the finding that this layer did not absorb water further after 6 months of storage in PBS (Fig. 2) may be the result of a process of crystallization occurring over time, particularly in the presence of biological fluids (12, 13, 22). This process is also known as maturation, which begins with an acid–base reaction initiated with depletion of metallic ions from the FAS glass by polyalkenoic acid and leaving siliceous hydrogel layers on the surface of the glass particles (27, 28). Subsequent formation of a poly-salt matrix within the set cement occurs as a result of the formation of cross-links between metallic ions and polyalkenoic acid (26–28). A final reaction that leads to the deposition of a silicate phase and the poly-salt compound contributes to the maturation of the absorptive layer (27–32). The results of this study confirmed that the maturation process occurs within the entire RMGIC layer.

However, the results of this study showed that such maturation processes might offer no protection against leakage and self-healing ability within the IDL of restorations after storage in PBS (Fig. 3A). YIU *et al.* (33) demonstrated that, even though specific GICs developed for the atraumatic restorative treatment of carious dentine may favour the penetration of particular ions deep into caries-affected dentine (23, 34), they fail to remineralize apatite-depleted dentine owing to a lack of nucleation of new apatite. The lack of remineralization has also been confirmed by KIM *et al.* (35) who reported the failure of a glass ionomer to remineralize apatite-depleted dentine, even in the presence of biomimetic remineralizing analogues. However, the ability of GIC to grow crystals (23), and the bioactivity of BAG (36–39) retained during the air-abrasion procedures (9, 36), may induce hydroxyapatite formation within the bonded-dentine interface, even in the absence of apatite nucleation (40), and protect the bond–dentine interface against the action of endogenous dentine proteases. Indeed, the RMGIC-bonded specimens stored in PBS for a period of 6 months presented important changes in terms of microporosity and nanoleakage in particular, when the bonded-dentine interfaces were created on Bioglass air-abraded dentine; dye diffusion (microporosity) was only observed along the dentine tubules with no uptake within the IDL (Fig. 3B).

SAURO *et al.* (37) recently demonstrated the ability of an air-abrasion BAG powder to remineralize the dentine via hydroxyapatite formation. The authors showed, using Raman spectroscopy, that completely demineralized dentine treated with Sylec Bioglass (OSspray, London, UK) and immersed in PBS for 48 h resulted in the reappearance of Raman peaks at 432 and 584 cm^{-1} and a high-intensity signal for hydroxyapatite at 961 cm^{-1} . The remineralization process induced by the Bioglass air-abrasion used in this study was caused by a simultaneous biomimetic process characterized by silicic acid $\text{Si}(\text{OH})_4$ release, and a poly-condensation reaction (38, 41). The presence of fluids analogous to saliva or body fluids (i.e. PBS) encouraged an immediate exchange between sodium ions (Na^+) and hydrogen cations (H^+ or H_3O^+), inducing a rapid release of calcium ions (Ca^{2+}) and phosphate (PO_4^{3-}) species from the particle structure (37, 39, 40). A modest, transient, increase in pH facilitated the precipitation of calcium and phosphate from the particles and from PBS to form an amorphous calcium phosphate layer ($\text{CaO-P}_2\text{O}_5$) that subsequently hydrolysed into hydroxyapatite as the reactions continued (39). The ability of GIC to grow crystals (23), the bioactive activity of BAG to induce hydroxyapatite precipitation, and the inactivation of endogenous proteases of dentine induced by remineralization processes gave such restorations a self-healing potential (42).

In terms of μTBS , the results of this study confirmed that the etching procedures performed with 10% PAA gel on the dentine surface before application of RMGIC favoured the establishment of bonded interfaces with a higher μTBS than when no PAA etchant was employed. Nevertheless, the creation of an RMGIC–dentine interface with the ability to maintain μTBS after prolonged

storage in PBS was only achieved when the bonding procedures were performed on dentine pretreated in a certain way (Table 3). Indeed, the μTBS of the RMGIC applied onto SiC-abraded dentine with (Group 1) or without (Group 2) the use of a PAA-etching gel, as well as the μTBS of the RMGIC applied onto BAG/ H_2O air-abraded PAA-etched dentine (Group 4) and BAG/PAA-fluid air-abraded dentine (Group 5), showed a statistically significant decrease ($P < 0.05$) after 6 months of storage in PBS. It is well known that acids may activate matrix collagenolytic (MMP-1, MMP-8, MMP-13) and gelatinolytic (MMP-2 and MMP-9) metalloproteinases (43–45). Therefore, the reason for this decrease in μTBS might be attributed to the exposure and activation of endogenous dentine metalloproteinases within the resin dentine as a result of PAA accumulation within the etched dentine surface and inside the dentinal tubules. In contrast, the RMGIC applied onto dentine surfaces air-abraded with BAG and H_2O followed by no PAA-etching procedure gave the lowest μTBS after 24 h (15.5 ± 17.3 MPa) and no statistically significant reduction in μTBS after 6 months of storage in PBS (12.5 ± 17.1 MPa). The reason why this type of bond–dentine specimen gave the lowest μTBS value at 24 h may be attributed to the lack of etching with PAA-gel before the bonding procedures, which allowed the RMGIC to create an exclusively chemical adhesion. Indeed, it is well known that the adhesion between GIC-based materials and dental hard tissues is achieved through an ionic exchange at the interface where the polyalkenoate chains enter the molecular surface of dental apatite, replacing phosphate ions (27). Calcium ions are displaced equally with the phosphate ions, leading to the development of an ion-enriched layer of cement that is firmly attached to the tooth (22). This sequence of reactions may have instead occurred with the Bioglass-rich dentine surface created during the air-abrasion procedures, creating a chemical bond between the RMGIC and the air-abraded dentine. Furthermore, the presence of Bioglass within the bonded interface may have stabilized the adhesion between dentine and RMGIC as a result of the creation of bioactive bonding via hydroxyapatite formation induced by BAG (37, 39) during the 6 months of storage in PBS. The application of RMGIC onto dentine surfaces air-abraded with BAG and 10% PAA fluid and subsequently etched with PAA gel-etchant favoured the establishment of high μTBS values at 24 h (36.5 ± 19.7 MPa) with no statistical reduction after 6 months of storage in PBS (32.1 ± 13.8 MPa). A possible explanation to justify the unique results obtained by the particular BAG/PAA combination may be that the 10% PAA fluid may have prewetted BAG particles during expulsion from the air-abrasion nozzle, facilitating their adhesion to the dentine surface. Moreover, the use of a PAA fluid and the further use of PAA etching-gel may also have facilitated subsequent chemical reactions among FAS, BAG, and collagen fibrils (30, 39, 46).

In conclusion, the air-abrasion procedures performed using a combination of BAG and PAA fluid, rather than BAG and H_2O , might increase the probability of BAG

particles embedding in dentine tubules and the dentine surface. The air-abrasion procedures performed using BAG and PAA fluid may also enhance the bonding durability of the RMGIC-bonded dentine when used according to the manufacturer's instructions (prior application of PAA etching gel). Furthermore, the air-abrasion pretreatment of the dentine surface executed using BAG may induce dentine remineralization and improve the healing ability of the restoration performed with RMGIC, satisfying the contemporary rationale of minimally invasive operative dentistry.

Acknowledgements – This article presents independent research commissioned by the National Institute for Health Research (NIHR) under the i4i programme and the Comprehensive Biomedical Research Centre at Guy's & St Thomas' Trust. The views expressed in this publication are those of the author(s) and not necessarily those of the NHS, the NIHR or the Department of Health. The authors also acknowledge support from the Centre of Excellence in Medical Engineering funded by the Wellcome Trust. The authors also acknowledge Dr. Laura Stipa from Dental School, University of Bologna, Italy and Peter Pilecki from Biomaterials, Biomimetics & Biophotonics (B3), King's College London Dental Institute, London, UK for their laboratory support.

Conflicts of interest – The authors have no financial affiliation or involvement with any commercial association with direct financial interest in the materials discussed in this manuscript. Any other conflict of interest is disclosed.

References

- BANERJEE A, WATSON TF. *Pickard's. Manual of Operative Dentistry*. Vol. 9. Oxford, UK: OUP Oxford, 2011.
- PETERS MC, MCLEAN ME. Minimally invasive operative care. II. Contemporary techniques and materials: an overview. *J Adhes Dent* 2001; **3**: 17–31.
- PETERS MC, BRESCIANI E, BARATA TJ, FAGUNDES TC, NAVARRO RL, NAVARRO MF, DICKENS SH. In vivo dentin remineralization by calcium-phosphate cement. *J Dent Res* 2010; **89**: 286–291.
- TAY FR, PASHLEY DH. Biomimetic Remineralization of Resin-bonded Acid-etched dentin. *J Dent Res* 2009; **88**: 719–724.
- BRESCIANI E, WAGNER WC, NAVARRO MF, DICKENS SH, PETERS MC. In vivo dentin microhardness beneath calcium-phosphate cement. *J Dent Res* 2010; **89**: 836–841.
- WANG Z, SA Y, SAURO S, CHEN H, XING W, MA X, JIANG T, WANG Y. Effect of desensitising toothpastes on dentinal tubule occlusion: a dentine permeability measurement and SEM in vitro study. *J Dent* 2010; **38**: 400–410.
- SEPULVEDA P, JONES JR, HENCH LL. In vitro dissolution of melt-derived 45S5 and sol-gel derived 58S bioactive glasses. *J Biomed Mater Res* 2002; **61**: 301–311.
- CERRUTI MG, GREENSPAN D, POWERS K. An analytical model for the dissolution of different particle size specimens of Bioglass in TRIS buffered solution. *Biomaterials* 2005; **26**: 4903–4911.
- SAURO S, WATSON TF, THOMPSON I. Dentine desensitization induced by prophylactic and air-polishing procedures: an in vitro dentine permeability and confocal microscopy study. *J Dent* 2010; **38**: 411–422.
- BANERJEE A, PAOLINELIS G, SOCKER M, MCDONALD F, WATSON TF. An in vitro investigation of the effectiveness of bioactive glass air-abrasion in the 'selective' removal of orthodontic resin adhesive. *Eur J Oral Sci* 2008; **116**: 488–492.
- PAOLINELIS G, WATSON TF, BANERJEE A. Microhardness as a predictor of sound and carious dentine removal using alumina air abrasion. *Caries Res* 2006; **40**: 292–295.
- HASHIMOTO M, NAKAMURA K, KAGA M, YAWAKA Y. Crystal growth by fluoridated adhesive resins. *Dent Mater* 2008; **24**: 457–463.
- ENDO K, HASHIMOTO M, HARAGUCHI K, OHNO H. Crystal growth by restorative filling materials. *Eur J Oral Sci* 2010; **118**: 489–493.
- NICHOLSON JW. Polyacid-modified composite resins ("compomers") and their use in clinical dentistry. *Dent Mater* 2007; **23**: 615–622.
- CZARNECKA B, LIMANOWSKA-SHAW H, NICHOLSON JW. Buffering and ion-release by a glass-ionomer cement under near-neutral and acidic conditions. *Biomaterials* 2002; **23**: 2783–2788.
- KERBY RE, BLEIHOLDER RF. Physical-properties of stainless steel and silver-reinforced glass-ionomer cements. *J Dent Res* 1991; **70**: 1358–1361.
- BEYLS HMF, VEREECK RMH, MARTENS LC, LEMAITRE L. Compressive strength of some polyalkenoates with or without dental amalgam alloy incorporation. *Dent Mater* 1991; **7**: 151–154.
- CATTANI-LORENTE MA, GODIN C, MEYER JM. Early strength of glass-ionomer cements. *Dent Mater* 1993; **9**: 57–62.
- WANG XY, YAP AUJ, NGO HC, CHUNG SM. Environmental degradation of glass-ionomer cements: a depth-sensing micro-indentation study. *J Biomed Mater Res* 2007; **82**: 1–6.
- CARDOSO MV, DELMÉ KI, MINE A, NEVES ADE A, COUTINHO E, DE MOOR RJ, VAN MEERBEEK B. Towards a better understanding of the adhesion mechanism of resin-modified glass-ionomers by bonding to differently prepared dentin. *J Dent* 2010; **38**: 921–929.
- SIDHU SK, WATSON TF. Resin-modified glass ionomer materials. A status report for the American Journal of Dentistry. *Am J Dent* 1995; **8**: 59–67.
- TOLEDANO M, OSORIO R, OSORIO E, AGUILERA FS, ROMEO A, DE LA HIGUERA B, GARCÍA-GODOY F. Sorption and solubility testing of orthodontic bonding cements in different solutions. *J Biomed Mater Res B Appl Biomater* 2006; **76**: 251–256.
- XIE D, ZHAO J, WENG Y, PARK JG, JIANG H, PLATT JA. Bioactive glass-ionomer cement with potential therapeutic function to dentin capping mineralization. *Eur J Oral Sci* 2008; **116**: 479–487.
- DE MUNCK J, VAN MEERBEEK B, YOSHIDA Y, INOUE S, SUZUKI K, LAMBRECHTS P. Four-year water degradation of a resin-modified glass-ionomer adhesive bonded to dentin. *Eur J Oral Sci* 2004; **112**: 73–83.
- SMALL ICB, WATSON TF, CHADWICK AV, SIDHU SK. Water sorption in resin-modified glass-ionomer cements: an in vitro comparison with other materials. *Biomaterials* 1998; **19**: 545–550.
- VERSLUIS A, TANTBIROJN D, LEE MS, TU LS, DELONG R. Can hygroscopic expansion compensate polymerization shrinkage? Part I. Deformation of restored teeth. *Dent Mater* 2011; **27**: 126–133.
- NICHOLSON JW. Chemistry of glass-ionomer cements: a review. *Biomaterials* 1998; **19**: 485–494.
- MCCABE JF. Resin-modified glass-ionomers. *Biomaterials* 1998; **19**: 521–527.
- MAEDA T, MUKAEDA K, SHIMOHIRA T, KATSUYAMA S. Ion distribution in matrix parts of glass-polyalkenoate cement by SIMS. *J Dent Res* 1999; **78**: 86–90.
- WASSON EA, NICHOLSON JW. New aspects of the setting of glass-ionomer cements. *J Dent Res* 1993; **72**: 481–483.
- SIDHU SK, SHERRIFF M, WATSON TF. The effects of maturity and dehydration shrinkage on resin-modified glass-ionomer restorations. *J Dent Res* 1997; **76**: 1495–1501.
- TAY FR, PASHLEY EL, HUANG C, HASHIMOTO M, SANO H, SMALES RJ, PASHLEY DH. The glass-ionomer phase in resin-based restorative materials. *J Dent Res* 2001; **80**: 1808–1812.
- YIU CK, TAY FR, KING NM, PASHLEY DH, SIDHU SK, NEO JC, TOLEDANO M, WONG SL. Interaction of glass-ionomer cements with moist dentin. *J Dent Res* 2004; **83**: 283–289.
- NGO H, MOUNT GJ, PETERS MC. A study of glass-ionomer cement and its interface with enamel and dentin using a low-

- temperature, high-resolution scanning electron microscopic technique. *Quintessence Int* 1997; **28**: 63–69.
35. KIM YK, YIU CK, KIM JR, GU L, KIM SK, WELLER RN, PASHLEY DH, TAY FR. Failure of a glass ionomer to remineralize apatite-depleted dentin. *J Dent Res* 2010; **89**: 230–235.
 36. PAOLINELIS G, BANERJEE A, WATSON TF. An in vitro investigation of the effect and retention of bioactive glass air-abrasive on sound and carious dentine. *J Dent* 2008; **36**: 214–218.
 37. SAURO S, THOMPSON I, WATSON TF. Effects of common dental materials used in preventive or operative dentistry on dentin permeability and remineralization. *Oper Dent* 2011; **36**: 222–230.
 38. NIU LN, JIAO K, QI YP, YIU CK, RYOU H, AROLA DD, CHEN JH, BRESCHI L, PASHLEY DH, TAY FR. Infiltration of silica inside fibrillar collagen. *Angew Chem Int Ed Engl* 2011; **50**: 11688–11691.
 39. HENCH LL, ANDERSSON Ö. Bioactive glasses. In: HENCH LL, WILSON J, eds. *Introduction to Bioceramics*. Singapore: World Scientific, 1993; 45–47.
 40. SEPULVEDA P, JONES JR, HENCH LL. Bioactive sol-gel foams for tissue repair. *J Biomed Mater Res* 2002; **59**: 340–348.
 41. ZHANG H, DARVELL BW. Synthesis and characterization of hydroxyapatite whiskers by hydrothermal homogeneous precipitation using acetamide. *Acta Biomater* 2010; **6**: 3216–3222.
 42. KIM YK, MAI S, MAZZONI A, LIU Y, TEZVERGIL-MUTLUAY A, TAKAHASHI K, ZHANG K, PASHLEY DH, TAY FR. Biomimetic remineralization as a progressive dehydration mechanism of collagen matrices—implications in the aging of resin-dentin bonds. *Acta Biomater* 2010; **6**: 3729–3739.
 43. PASHLEY DH, TAY FR, YIU C, HASHIMOTO M, BRESCHI L, CARVALHO RM, ITO S. Collagen degradation by host-derived enzymes during aging. *J Dent Res* 2004; **83**: 216–221.
 44. NISHITANI Y, YOSHIYAMA M, WADGAONKAR B, BRESCHI L, MANNELLO F, MAZZONI A, CARVALHO RM, TJÄDERHANE L, TAY FR, PASHLEY DH. Activation of gelatinolytic/collagenolytic activity in dentin by self-etching adhesives. *Eur J Oral Sci* 2006; **114**: 160–166.
 45. BRESCHI L, MAZZONI A, NATO F, CARRILHO M, VISINTINI E, TJÄDERHANE L, RUGGERI A JR, TAY FR, DORIGO EDE S, PASHLEY DH. Chlorhexidine stabilizes the adhesive interface: a 2-year in vitro study. *Dent Mater* 2010; **26**: 320–325.
 46. DAY RM, BOCCACCINI AR, SHUREY S, ROETHER JA, FORBES A, HENCH LL, GABE SM. Assessment of polyglycolic acid mesh and bioactive glass for soft-tissue engineering scaffolds. *Biomaterials* 2004; **25**: 5857–5866.